

## **Chapter 2**

### **Synthesis and characterization techniques**

*This chapter includes the details of the cost-efficient and environment-friendly synthesis process used to synthesize the phosphors and nanocomposites used in the thesis. The details of the characterization tools and the instruments used for characterization are also discussed in this chapter.*



### 2.1 Overview

This chapter describes the detailed methodology of the sample preparation and experimental tools involved in the characterization of the prepared samples. In the present investigation, the samples were synthesized by the urea-assisted auto-combustion and co-precipitation methods. This chapter also provides a brief description of the apparatus and the procedure used for characterization. The chapter starts with the techniques and steps required in the synthesis of doped Bi<sub>2</sub>O<sub>3</sub> and ZnO based low-dimensional materials, followed by a discussion on the experimental techniques employed for the investigation of their structural, optical and electrical properties.

### 2.2 Sample preparation

#### 2.2.1 Co-precipitation method

In the chapters 3, 4, and 6, the co-precipitation method was employed for the preparation of doped and co-doped Bi<sub>2</sub>O<sub>3</sub> phosphors and also for the synthesis of ZnO based nanocomposites. This is an important and widely used synthesis route in preparation of many inorganic polycrystalline samples. Briefly, in a typical synthesis of Sm<sup>3+</sup>/Li<sup>+</sup> co-doped Bi<sub>2</sub>O<sub>3</sub> phosphor, the stoichiometric amount of rare-earth nitrates, bismuth nitrate pentahydrate, and precursors of other dopants were taken in a clean vessel with double-distilled water in it. The solution was constantly stirred for 1 hour on a magnetic stirrer at 50 °C. To eliminate the surplus acid, the mixture was constantly heated. In order to obtain a transparent solution, HNO<sub>3</sub> was added dropwise. Desired quantity of samarium nitrate was added with continuous stirring. A stoichiometric amount of lithium acetate was taken in another beaker and HNO<sub>3</sub> was added drop-wise to ensure the formation of lithium nitrate. Both the reaction mixtures were combined in a single beaker. 2M NaOH was added drop-by-drop to ensure complete precipitation. The reaction mixture was left overnight to settle down. The resulting white precipitate was washed repeatedly with DI

water and allowed to dry at 80 °C overnight and then calcined in air at 600 °C for 4hrs and we obtained a bright yellow powder.

Similarly, for the synthesis of ZnO nanoparticles, the stoichiometric amount of  $Zn(NO_3)_2 \cdot 6H_2O$  was dissolved in 200 ml of DI water under constant stirring for 1 hour at ambient conditions. A pH value of ~8 was achieved by drop-wise mixing of NaOH solution and then solution was left for precipitation overnight. The obtained white precipitate was washed 3-4 times with DI water and ethanol followed by drying in an oven at 90 °C for 12hrs and then annealed for 2 hrs at 550 °C. Now, to synthesize Ag-ZnO nanocomposites, the prepared ZnO nanoparticles and  $AgNO_3$  powder were mixed with desired amount of ethylene glycol and vigorously stirred at room temperature for 1 hr to obtain a homogeneous mixture. The obtained brown precipitates were washed, dried (at 90 °C for 12 hrs) and annealed in air and 550°C for 2 hrs. The flow chart for synthesis of ZnO nanoparticles and Ag-ZnO nanocomposites are depicted in Figs. 2.1 (a, b).

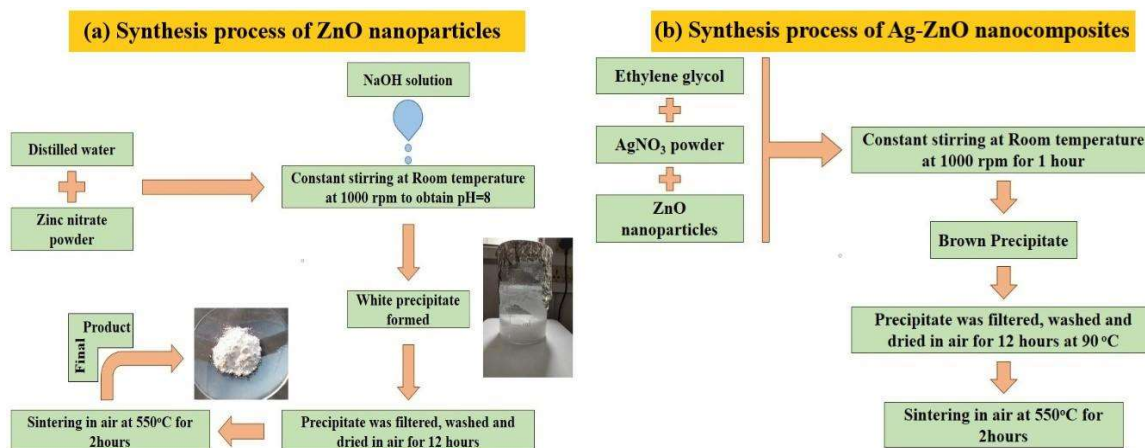


Fig. 2.1 Flow chart for the synthesis of (a) ZnO nanoparticles and (b) Ag-ZnO nanocomposites.

### 2.2.2 Urea-assisted auto combustion method

In chapter 5, the urea assisted auto-combustion method was used for the preparation of doped and co-doped  $Bi_2O_3$  phosphors. In this method, the stoichiometric proportion of

rare-earth nitrates and bismuth nitrate pentahydrate were taken in a clean beaker and desired amount of nitric acid was added in it. The solution was constantly stirred at 50 °C for 1 hour to get a homogeneous solution. Calculated amount of urea was added to this solution and stirring was continued to ensure proper mixing. Now, the temperature was raised to 250 °C and the reaction mixture was left for 12 hours for combustion. The obtained material was grinded and powdered and then calcined in a furnace at 600 °C for 4 hours.

### 2.3 Characterizations techniques & their working principles

The techniques utilized to investigate the structural and optical characteristics of the materials are listed below and detailed descriptions in different sections.

- ❖ Structural properties: X-ray diffraction, X-ray photoelectron spectroscopy, and Fourier transform infrared spectroscopy.
- ❖ Elemental analysis: Energy dispersive X-ray spectroscopy.
- ❖ Surface morphology: High-resolution scanning electron microscopy.
- ❖ Particle distribution: Transmission electron microscopy.
- ❖ Absorption properties: UV-Vis spectroscopy.
- ❖ Photoluminescence properties: Photoluminescence excitation and emission spectroscopy, Photoluminescence decay analysis, Temperature-dependent photoluminescence properties.
- ❖ Electrical properties: I-V curve and photoresponse measurements.

### 2.3.1 X-ray diffraction:

X-ray diffraction (XRD) is a primary non-destructive analytical technique used for identification and quantification of the crystal structure and phase purity of the crystalline/polycrystalline materials. It is also helpful in determining crystallite size and lattice strain of the samples. The XRD plots are also used to fetch refined atomic positions, lattice parameters, bond angles, and bond lengths after the Rietveld refinement. The Rigaku-MiniFlex 600 desktop X-ray diffraction system, operating at 30 kV and 15 mA was used to record the XRD patterns of the powdered phosphors. The system is equipped with a 600 W Cu  $K_{\alpha}$  radiation source ( $\lambda=1.5418 \text{ \AA}$ ), NaI scintillation counter detector, and graphite monochromator. The X-ray diffractometer and the schematic representation of X-ray diffraction are presented in Figs. 2.2 (a) and (b), respectively.

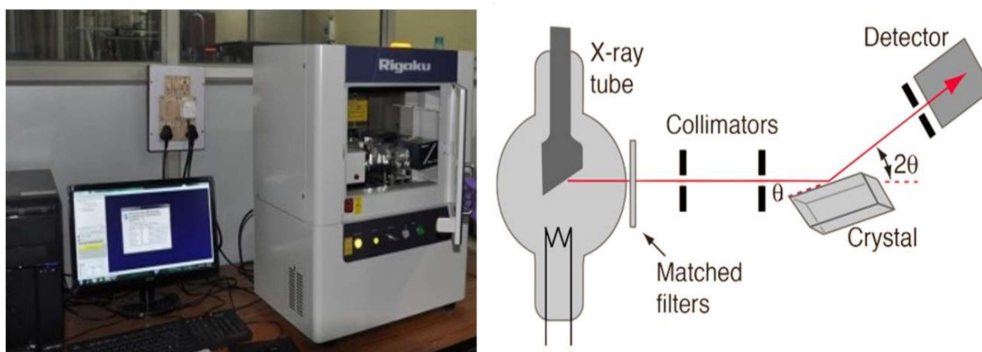


**Fig. 2.2 (a)** Rigaku-MiniFlex-II DESKTOP powder X-ray diffractometer set up **(b)** Schematic representation of X-ray diffraction.

When an incoming beam of X-ray radiation strikes with the powder sample, diffraction occurs in every conceivable direction of  $2\theta$ , as illustrated in Fig. 2.2 (b). A movable detector (NaI scintillation counter) linked to a chart recorder is used to detect the diffracted beam. The intensity of the diffracted beam as a function of the incident angle is called “diffraction pattern”. In normal operation, the counter is configured to scan over a range of  $2\theta$  values at a constant angular velocity. Generally, a  $2\theta$  range of 10 to 90 degrees is enough to cover the important aspect of the specimen’s crystal information.

The identification of single or multiple phases aids in understanding the mechanism of sample formation.

The formulation of the XRD was first proposed by Sir Lawrence Bragg and Sir William Henry Bragg in 1913. They discovered that crystalline solids produce intense peaks of reflected radiation at specific wavelengths and incident angles. When a crystalline solid is bombarded with X-ray radiation of a wavelength comparable to the atomic spacing of the crystal lattice planes ( $d$ ) and at a certain incident angle ( $\theta$ ), intense reflected X-rays are produced when the wavelength of the scattered X-rays ( $\lambda$ ) interfere constructively. When the difference in the travel path is equal to the integral multiple of the wavelength, the scattered waves interfere constructively. When constructive interference occurs, a diffracted beam of X-rays will leave the crystal at an angle equal to that of the incident beam. The condition for constructive interference is given by Bragg's law,

$$2d\sin\theta = n\lambda \quad (2.1)$$

When the incident radiation satisfies the Bragg's law, the diffracted beam will make coherent superposition and a maximum intensity can be recorded using a detector. The schematic illustration of Bragg's diffraction from the crystal lattice planes is depicted in Fig. 2.3.

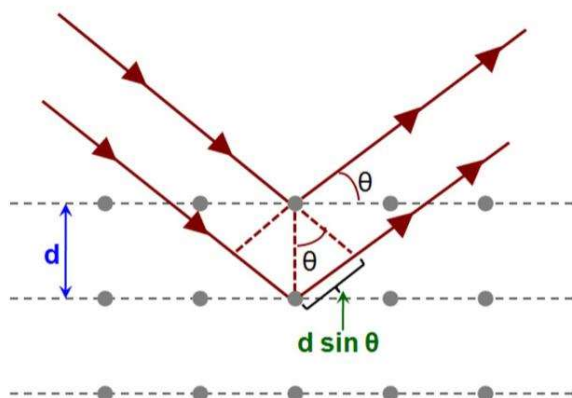


**Fig. 2.3** Schematic illustration of Bragg's diffraction of X-rays from atomic planes.

### 2.3.2 High resolution Scanning electron microscope (HR-SEM) and Energy dispersive X-ray spectroscopy (EDX)

The HR-SEM is an instrument used to provide a wide variety of informations such as morphology, shape, grain size, and orientation of the components from the sample surface. The EDX is employed for both qualitative and quantitative confirmation of all the elements present in the sample. The Nova Nano SEM 450, FEI Company of USA (S.E.A.) PTE, LTD set used for HR-SEM and EDX analysis is shown in Fig. 2.4. HR-SEM is also termed as FE-SEM (Field emission scanning electron microscopy). It follows the same principle as that of SEM. The biggest difference between a FE-SEM and a SEM lies in the electron generation system. In FE-SEM the electrons are emitted. The interaction of an electron beam with an atom at various depths within a sample generates different signals such as the secondary electrons, characteristic X-ray, backscattered electrons, cathodoluminescence, transmitted electrons, and absorbed current (specimen current). The signals are used by HR-SEM to produce an image. Detecting all signals in an instrument is difficult. The standard equipment in all HR-SEM is a secondary electron detector. Secondary electron imaging detects the secondary electrons that are released from the top surface of the specimen. HR-SEM examination can be used to get very high-resolution images of a specimen's surface. Backscattered electrons are beam electrons that are reflected off a material due to elastic scattering. The resolution of backscattered electrons (BSE) is less than the secondary electron due to its origin from deeper locations within the specimen. The strength of the BSE signal is highly connected to the specimen's atomic number ( $Z$ ), thus BSE pictures may be utilized to get information about the distribution of various elements in the sample. The sample in powder, as well as, palette form can be used for HR-SEM analysis.

EDX spectroscopy is used to get information about the presence of an element as well as the atomic and weight percentage of an element in the sample. The energy-dispersive spectrometer measures the energy and amount of X-rays released by the material as a result of an energy difference between the higher and lower-energy shells. Since the energies of the X-rays are typical of the atomic structure of the emitting element and the energy difference between the two shells. Therefore, EDX may be used to determine the elemental makeup of the sample. The EDX is equipped with an HR-SEM setup.



**Fig. 2.4** HR-SEM and EDS set up.

### **2.3.3 Transmission Electron Microscopy (TEM)**

Transmission electron microscopy (TEM) is a microscopic technique in which a highly focused electron beam is incident on a very thin sample, transmits through it and provides a high resolution image. An imaging device, such as a fluorescent screen or sensor like a CCD camera, is used to magnify and focus this image. TEM image reveals information about morphology, crystallography and particle size distribution with a spatial resolution of approximately 1 nm. The small de Broglie wavelength of the incident electrons makes it possible for the extraordinary magnification range, which is essential to the distinctive

capabilities of TEM imaging and enables the instrument to study minute features, down to a single column of atoms. A TEM setup consists several components such as an electron gun to generate the electron stream, a vacuum system in which the electrons travel, voltage generator, a series of electromagnetic lenses, recording devices, as well as electrostatic plates. TEM is used in all major areas of science including material as well as biological sciences. A thin carbon film with a thickness and mesh size ranging from a few to 100  $\mu\text{m}$  and supported on a 3 mm diameter carbon coated copper grid is used as a sample holder. The sample required for TEM analysis is prepared by dispersing the synthesized phosphors in ethanol. The properly dispersed sample is placed over the inner meshed area having the diameter of approximately 2.5 mm. Generally, grid materials are copper, molybdenum, gold or platinum. This grid is fitted into the sample holder, which is connected to the specimen stage. Depending on the type of experiment being executed, a wide range of stage and holder designs are available. TEM microscopy can be divided into two classes on the basis of electron recording by detector, that is bright-field and dark-field microscopy. Among them, bright field imaging mode is the most common mode of operation for TEM. In this mode, the contrast is due to occlusion and absorption of electrons in the sample (classically). Thicker area of the sample or region with a higher atomic number appears dark, whilst region with no sample in the beam path appears bright. The TEM images have been recorded with TECNAI G2 20 TWIN (FEI) Transmission Electron Microscope to investigate morphology and particle sizes of samples (Fig. 2.5). The copper grid with 300 meshes has been used for TEM sample measurement.

Selected area electron diffraction (SAED) is an experimental technique that is performed alongwith the TEM and used to identify the crystal structure and measure the crystallinity, lattice parameters, and orientation of the samples. In a TEM, a thin

crystalline specimen is exposed to a beam of high-energy electrons. As TEM specimens are typical  $\sim 100$  nm thick, and the electrons typically have the energy of 100-400 keV, the electrons pass through the sample easily. Since the wavelength of high-energy electrons is a fraction of a nanometer and the separation between atoms in a solid is only slightly greater, the atoms act as a diffraction grating to the electrons. This means that some atoms will be scattered to specific angles given by the crystal structure of the sample, while others will pass through the sample undeflected. Consequently, TEM will display a series of spots on the screen. In the SAED pattern, each spot corresponds to a satisfied diffraction condition of the sample's crystal structure. Sharp diffraction spots indicate lattice reflections in SAED patterns, which are projections of the reciprocal lattice.



**Fig. 2.5** Transmission electron microscope

### 2.3.4 Fourier Transform Infrared (FTIR) Spectroscopy

The FTIR spectrum was utilized to learn about inter or intramolecular interaction, functional groups, and vibrational modes. FTIR spectroscopy is employed to collect an infrared spectrum of absorption, emission, and infrared inelastic scattering of a sample (solid, liquid, or gas). It is one of the most powerful techniques used for chemical identification, quantitative analysis and structural analysis of chemical substances. In this spectroscopic technique infrared radiations are used as source to detect the vibrational modes present in the samples. FTIR spectrometer obtains spectral data in a wide spectral range. This gives it a substantial edge over other spectrometers that measure intensity across a limited range of wavelengths at a time. The FTIR approach has overcome the limitations encountered with dispersive infrared spectrometers and opened up new possibilities for infrared spectroscopy. The phrase Fourier transform in FTIR spectroscopy refers to the process of converting raw data into an actual spectrum using a Fourier transform (a mathematical method). The schematic diagram for an FTIR spectrometer is shown in Fig 2.6 (b). The horizontal axis represents the mirror's location, while the vertical axis represents the amount of light measured. This is the "raw data" from which a spectrum can be generated.

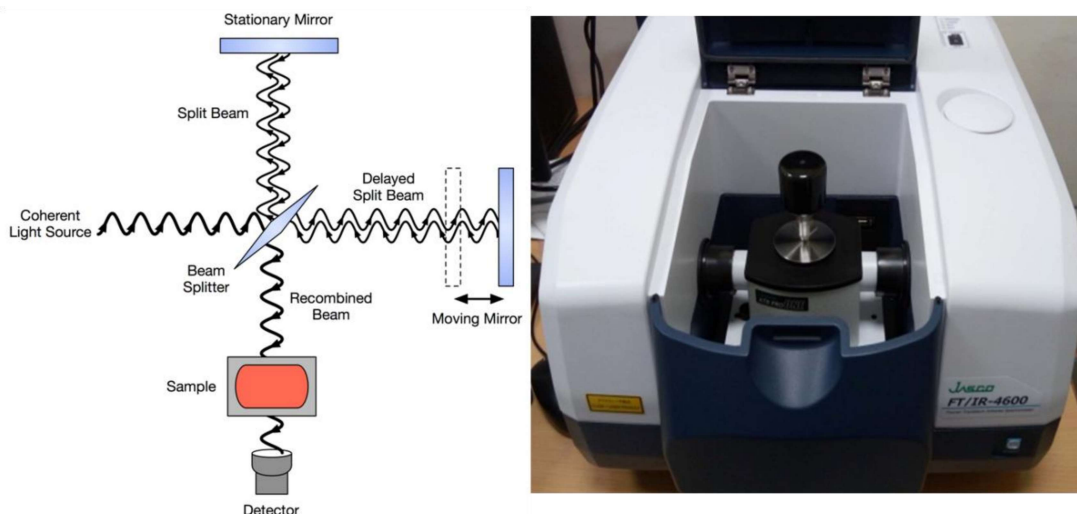


**Fig. 2.6 (a)** Working principle of FTIR, and **(b)** JASCO 4600 FTIR spectrometer.

A light source produces the beam, which contains the whole range of wavelengths to be examined. The FTIR spectrometer contains a Michelson interferometer, attired with a combination of two mirrors and a beam splitter. One of the mirrors is fixed whereas one of them is movable. For each new data point, the beam is adjusted by changing one of the mirrors, which alters the set of wavelengths that pass through. Light from the source is collimated and routed to a beam splitter in a Michelson interferometer. The interferometer produces a unique type of signal which has all of the infrared frequencies “encoded” into it. The signal can be measured very quickly, usually on the order of one second or so. Thus, the time element per sample is reduced to a matter of a few seconds rather than several minutes. Ideally, 50% of the light is reflected towards the fixed mirror and 50% is transmitted towards the moving mirror. The light is reflected back to the beam splitter by the two mirrors, and (ideally) 50% of the original light enters the sample compartment. Here the light is focused on the specimen. The light is refocused on the detector as it exits the sample chamber. The FTIR data for the thesis work was taken from the Jasco FT/IR-4600 spectrometer equipped with a  $45^{\circ}$  Michelson interferometer, High-intensity ceramic source, and D1aTGS detector. The sample measurement was performed using attenuated

total reflectance (ATR) accessory facilitated with a diamond ATR prism. The key advantage of the ATR-FTIR setup (Fig. 2.7) is that it requires no special sample preparation before spectral measurement as the penetration depth of IR radiation in the sample with ATR measurements is independent of sample thickness. Another advantage is that because of the limited path length in the sample, the strong attenuation of the IR signal in highly absorbing media is avoided.

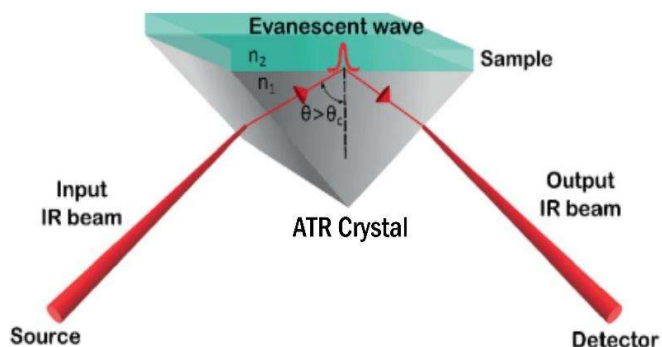


Fig. 2.7 Illustration of the mechanism behind ATR setup

### 2.3.5 X-ray photoelectron spectroscopy (XPS)

XPS is a quantitative spectroscopic and surface-sensitive technique. It is a powerful technique used to collect chemical information about the surfaces of solid materials viz., oxidation states, elemental composition, ligand coordination, etc. which is required for explanation of different physical/chemical properties of samples. It is also used to identify the active sites, surface contamination or dust on the samples, oxide layers on non-oxide materials, etc. Insulators and conductors may both be examined in surface depths ranging from a few microns to a few millimeters. The XPS is used as a surface-sensitive tool since it mainly identifies those electrons produced near the surface. The kinetic energy of the photoelectrons is quite low. As a consequence of the inelastic collisions in the sample's atomic structure, photoelectrons generated more than 20 to 50 Å beneath the surface do not have sufficient energy to be detected in this technique. The XPS technique is based on the concept of Einstein's photoelectric effect. The sample under investigation is kept inside an

ultrahigh vacuum ambiance (typically  $\sim 10^{-10}$  torr) and then it is exposed to a monochromatic, low-energy X-ray source. The X-rays incident on the sample results in the ejection of core-level electrons from sample atoms. These ejected beam of electrons is analysed, and thus XPS is a type of electron spectroscopy, also known as ESCA (electron spectroscopy for chemical analysis). If a photon of energy  $h\nu$  falls on the surface of the sample and an electron from the inner shell gets ejected by absorbing this photon then the kinetic energy (K.E.) of this electron, detected at the analyzing unit of XPS instrument is given by,

$$\text{K. E.} = h\nu - \text{B. E.} - \Phi \quad (2.2)$$

Where, B.E. is the binding energy of the ejected electrons and  $\Phi$  is the work function of spectrometer of instrument. The energy of a core electron produced in such a photoemission process is a function of its binding energy and is a characteristic of the element from which it was emitted. The primary data used for XPS is the energy analysis of the photo-emitted electrons. An outer electron occupies the position of a core hole after the incoming X-ray ejects the core electron. By the emission of an Auger electron or a characteristic X-ray, these energies get compensated. Further, in XPS Auger electron's energy can also be utilized along with the emitted photoelectrons. Fig. 2.8 (a) depicts the schematic representation of XPS instrumentation. The Thermo scientific K- alpha XPS setup was employed to perform elemental analysis and chemical state of the compositions and is shown in Fig. 2.8 (b). The various components of XPS are listed as,

**i) Source:** The photon source in XPS is usually X-ray radiation from an Aluminium or magnesium target. In our measurement, the X-ray source used in the setup is monochromatic Aluminium (Al) K-alpha X-ray. A monochromator is used to reduce the band width of X-ray photons, which provides a very small spot on the sample surface.

**ii) Sample holder:** Here sample (to be examined) is placed which lies between the entrance slit of spectrometer and source. The zone around the sample holder is kept at ultrahigh vacuum ( $\sim 10^{-10}$  torr).

**iii) Analyzer:** The analyzer is hemispherical in shape and kept in a very high static electric field. The electrons entering into the analyzer follows a curved route with curvature depending on the strength of the electric field and their K.E.

**iv) Detector:** It is placed where the electrons are multiplied and converted into a pulse of electrons.

**v) Signal processor and read out:** This unit amplifies the signals and converts it into a spectrum.

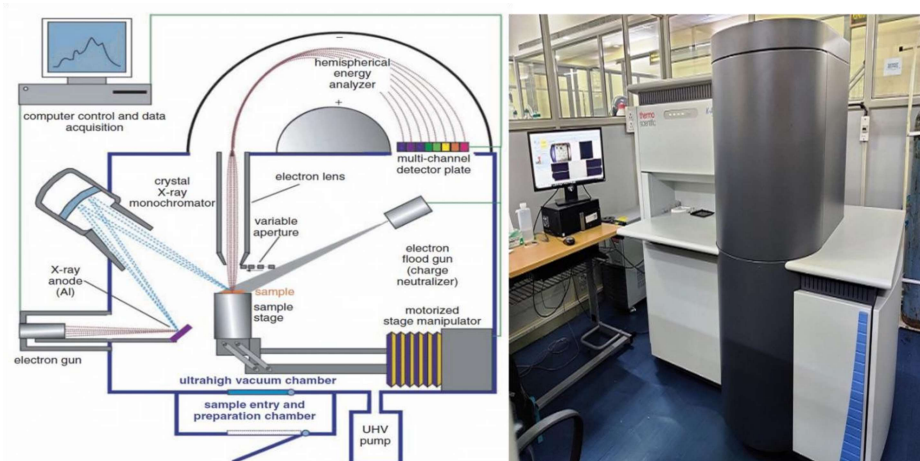


**Fig. 2.8 (a)** Schematic representation of the XPS instrumentation and **(b)** Thermo scientific K- alpha XPS setup.

### 2.3.6 UV-Vis Absorption Spectroscopy

Ultraviolet-Visible (UV-Vis) absorption spectroscopy is an extensively employed analytical method that determines the wavelength of the incident photons that are transmitted through or absorbed by a specimen in contrast to a blank or reference. This feature is impacted by the sample composition, possibly giving information about the sample and its concentration. It is a versatile technique employed for measurement of the optical band gap of materials. Moreover, the applications of UV-Vis spectroscopy lies in

the identification of the charge transfer transitions which results in the broad absorption spectrum, validation of the defect trap states formed within the bandgap, photocatalysis, in the field of the pharmaceutical industry where absorbance peaks help to identify individual pharmaceutical compounds, to identify the constituents of a substance, determine their concentrations, to identify functional groups in molecules, and many more.

### 2.3.6.1 UV-Vis spectrophotometer

The UV-Vis spectrophotometer is the equipment used to record the absorption spectra of the samples. The absorption analysis of all the samples related to the thesis work is performed with the help of the Jasco V-770 UV-Vis-NIR spectrophotometer (Fig. 2.9). The spectrophotometer consists of four main components namely a radiation source, a sample holder compartment, a monochromator (diffraction grating), and a detector. The Jasco V-770 spectrophotometer consists of two radiation sources, a deuterium arc lamp as a UV source (190 to 400 nm) and a Halogen lamp as a visible and NIR source (300 to 2500 nm). A photomultiplier tube (PMT) has been used as a detector to detect the UV and visible radiations. A 60 mm UV-Vis integrating sphere is employed to analyze the absorption spectrum of powdered samples. The inner surface of integrating sphere is coated with barium sulphate as it reflects the incident UV and visible radiations. The scanning monochromator "steps across" each wavelength, allowing the intensity to be measured as a function of wavelength.

### 2.3.6.2 UV-Vis spectroscopy analysis

The measurement of absorption spectra of the powdered samples is performed using an integrating sphere setup installed in the sample compartment of the spectrophotometer. The integrating sphere has an opening where the solid sample holder with the sample is kept for measurement and another opening for light to enter the sphere. Before the sample

measurement, the baseline measurement is conducted by closing the opening of the integrating sphere with the barium sulphate chalk. After the baseline measurement, the sample is placed in a holder at the opening in the integrating sphere. The absorbance ( $A$ ) is equated by taking the logarithm of a fraction involving the intensity of light before passing through the specimen ( $I_0$ ) divided by the intensity of light after passing via the specimen ( $I$ ). Transmittance ( $T$ ) is defined as the fraction of  $I$  divided by  $I_0$ , which represents the amount of light passing via the specimen.

$$A = \log_{10} \left( \frac{I_0}{I} \right) = \log_{10} \left( \frac{1}{T} \right) = -\log_{10}(T) \quad (2.3)$$



**Fig. 2.9** UV-Vis spectrophotometer (Jasco V-770) equipped with an integrating sphere setup.

### 2.3.7 Photoluminescence Spectroscopy

Photoluminescence (PL) spectroscopy is a non-destructive, non-contact, and powerful technique to probe the luminescence property of a specimen. Fundamentally, light is focused onto the specimen, followed by its absorption and the process is known as photo-excitation. The photo-excitation results in the compound jumping to the excited electronic state and eventually releasing photons (energy) when it relaxes and returns to a lower energy level. PL is the emission of photons or luminescence caused by this mechanism. Typically, the duration between absorption and emission is quite brief. The quantum mechanics rules are used to determine the allowed transitions

between states. A fundamental principle is understood by examining the electron configurations and molecular orbital of basic molecules and atoms. Typical applications of the PL measurement include the determination of the luminescence phenomenon such as PL emission and excitation, bandgap determination, impurity levels, defect detection, molecular structure and crystallinity, recombination mechanism, and energy transfer processes.

### 2.3.7.1 PL spectrophotometer

The schematic diagram of the spectrophotometer employed in the thesis work is depicted in Fig 2.10 (a). The spectrophotometer used is Horiba fluorolog-3 (Fig 2.10 (b)) which is fitted with a xenon arc lamp as an excitation source, two single grating monochromators at the excitation and emission ends, and a detector comprising a photomultiplier tube. The excitation monochromator consists of two gratings, which decrease stray light, that is, light with frequencies different from the selected one. To reduce stray light, these monochromators employ concave gratings created using holographic techniques. Both monochromators are motorized, allowing for automated wavelength scanning. Fluorescence is detected and measured using the proper electrical instruments. The output is often displayed graphically and digitally preserved.

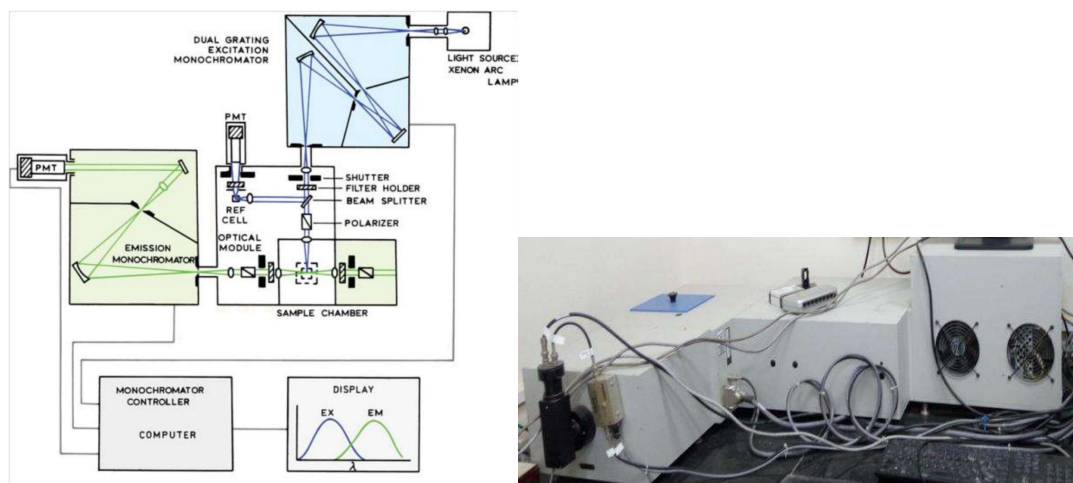


**Fig. 2.10 (a)** Components and working ray diagram of PL spectrophotometer setup **(b)** Horiba Photoluminescence spectrophotometer.

### 2.3.7.2 PL Lifetime measurement

The PL lifetime measurement is employed either in the frequency domain or time domain. The time domain approach includes illuminating a specimen with a short pulse of light and then measuring the intensity of the emission versus time. The slope of the decay curve is then used to calculate the PL lifespan. A fluorophore's PL lifespan is an inherent attribute. Fluorophore concentration, specimen thickness, specimen absorption, method of measurement, photo-bleaching, fluorescence intensity, and/or excitation intensity do not affect PL lifespan. PL lifetime is sensitive to internal factors that are dependent on fluorophore structure.

### 2.3.7.3 Temperature-dependent PL measurement

The temperature-dependent PL analysis was performed using the same spectrophotometer. The sample was first prepared in pallet form and was then placed in the modified sample holder coupled with a heating element and temperature sensing device. The temperature was controlled by the external temperature controller. The temperature-dependent PL measurements of the samples in chapters 4 and 5 were carried out using this setup.

## 2.8 Current-Voltage characteristics and responsivity measurements

The current-voltage (I-V) characteristics of the samples have been obtained using a source meter (model B1500A from Keysight, USA) and UV lamp ( $\lambda=365$  nm) in the range -2 V to 2 V at room temperature under ambient air environment. Responsivity is one of the main characteristics of the photodetectors and can be calculated using the formula,

$$R = \frac{I_{light} - I_{dark}}{P * S} \quad (2.4)$$

Where,  $I_{\text{dark}}$  and  $I_{\text{light}}$  denote the dark and photo-currents, respectively.  $P$  stands for the optical power density and an effective area of the device is denoted by  $S$ .



**Fig. 2.11** I-V measurement setup.

